J Mater Sci (2009) 44:6538–6545
DOI 10.1007/s10853-009-3709-z

MESOSTRUCTURED MATERIALS

Organic solvent treatment and physicochemical properties of nanoporous polymer–SBA-15 composite materials

Magali Wainer · Louis Marcoux · Freddy Kleitz

Received: 30 November 2008 / Accepted: 24 June 2009 / Published online: 10 July 2009

Abstract Mesoporous polymer–silica composites are attractive new materials because these systems can combine the advantages of highly porous silica and the vast functional diversity of organic polymers in a single robust structure. This contribution deals with the effects of organic solvent treatment on the physicochemical properties of mesostructured polymer–SBA-15 silica nanocomposites. For this study, two distinct reference mesoporous nanocomposites were prepared using a previously reported surface-confined polymerization technique, e.g., poly(styrene) (PS)–SBA-15 composite and poly(2-hydroxyethyl methacrylate)(PHEMA)–SBA-15 composite. The resulting materials are treated either with chloroform or toluene under heating for a prolonged period of time (24 h). Both materials are characterized prior and after solvent treatment by nitrogen physisorption at −196 °C, thermogravimetry and Attenuated Total Reflection Infra-Red (ATR-IR) spectroscopy. In general, solvent stability is excellent for both types of composite, even for low cross-linking degree of the polymer. Our data reveal that a treatment of mesoporous PHEMA–SBA-15 with chloroform or toluene has a minor, but reproducible, effect on the composite material in terms of porosity. Here, a reorganization of the polymer layer–silica interface seems to occur to some extent, which is leading to slight variation of the intrawall porosity. As a consequence, an increase of the thermal stability is clearly observed, with, however, no marked difference in the mean mesopore diameter. On the other hand, the PS–SBA-15 composite treated with the same solvents shows higher specific surface area values and an improved homogeneity in terms of polymer coating compared to untreated materials, especially for composites synthesized using benzoyle peroxide as the polymerization initiator. However, no increase in thermal stability is observed in this case.

M. Wainer · L. Marcoux · F. Kleitz (✉)
Canada Research Chair on Functional Nanostructured Materials, Department of Chemistry, Université Laval, Quebec, QC G1V 0A6, Canada
e-mail: freddy.kleitz@chm.ulaval.ca

Introduction

To design mesostructured materials [1, 2] for applications in liquid-phase heterogeneous catalysis [3–5], separation [6], and immobilization or controlled release of bioactive compounds [7, 8], the introduction of specific organic functions is often a crucial step [9–13]. To do so, the inclusion of organic polymers in mesoporous silica has been proposed as an interesting alternative [14–19] to more classical strategies which are widely adopted to functionalize mesoporous silica, namely post-grafting of functional organosilanes and co-condensation methods. In particular, the mesopore surface-confined polymerization approach developed by Choi et al. [20] appears as a versatile method to introduce diverse organic functionalities with a control of the spatial location and tailored functional site densities. In this strategy, specific vinyl-based monomers are selectively polymerized inside large pore silica (e.g., SBA-15-type silica [2]). Precisely, the monomers are polymerized while being adsorbed on the mesopore surface, forming ultimately a thin polymeric coating on the mesopore walls. Several research groups have already taken advantage of this approach in the recent years to develop new functional materials [21–24]. Also, it has been shown that these mesostructured polymer–silica composites can further be functionalized by reacting suitable molecular species with the mesoporous polymer surface [20, 25]. However, the effects of such post-polymerization treatments on the

properties of the polymer coating remain to be examined in details. In this contribution, we investigate the solvent stability of the materials, with emphasis on the effects observed upon prolonged exposure of the composites to polar and non-polar organic media. For our investigations, we selected two systems: (1) polymer–SBA-15 composites synthesized with the hydrophilic 2-hydroxyethyl methacrylate monomer, (PHEMA), and (2) polymer–SBA-15 composites prepared with the apolar styrene monomer (PS). The resulting mesoporous materials are treated with chloroform or toluene solutions under heating for a period of 24 h. All materials are characterized before and after the solvent treatment using nitrogen physisorption at −196 °C, thermogravimetric analyses and ATR-IR spectroscopy. These techniques are shown here to be particularly suited for the characterization of the porous composites under investigation. In particular, distinct effects on the materials porosity are revealed depending on the nature of the polymer and type of solvent.

Experimental

Materials

High quality mesoporous SBA-15 silica host was synthesized using the procedure proposed by Choi et al. [26]. In a typical SBA-15 synthesis, 18.46 g of P123 (Aldrich) was dissolved in a mixture of 331.00 g H_2O and 10.30 g HCl (37 wt%, Fisher). The clear solution was then stirred at 35 °C for 1 h before addition of 29.76 g of TEOS (98%, Aldrich). The reaction was carried out with vigorous stirring at 35 °C for 24 h. Subsequent hydrothermal treatment was performed at 100 °C for 48 h. The resulting powder was then filtered and dried at 100 °C for 24 h. Extraction of the structure-directing agent was performed in an acidic EtOH solution followed by calcination in air at 550 °C for 5 h. The mesoporous composites were synthesized according to the procedure reported by Choi et al. [20]. For the present study, the monomers used were 2-hydroxyethyl methacrylate, HEMA (Aldrich, 97%) and styrene, Sty (Alfa Aesar, 99%). Polymer loading was kept constant at 30 wt%, and three different cross-linking degrees, 20, 5 and 2% were applied by introducing ethyleneglycol dimethacrylate (EDMA, Sigma-Aldrich, 97%) and divinylbenzene (DVB, Aldrich, 80%), for PHEMA and PS, respectively. Benzoyle peroxide, BPO (Aldrich, 97%), was used as radical initiator in the case of PHEMA, and both BPO or 4,4′-azoisobutyronitrile, AIBN (Laboratoires Mat, 98%), were used in the case of PS. In a typical PHEMA–SBA-15 synthesis with 20% cross-linking, 217 mg HEMA, 83 mg EDMA, and 18 mg BPO were first dissolved in 1.9 mL of CH_2Cl_2 (Fisher, 99.9%). The mixture was then introduced into 1.0 g SBA-15 (outgassed overnight at 150 °C under vacuum) using the incipient wetness technique. CH_2Cl_2 was then evaporated at 35 °C for 4 h, followed by vacuum-freeze thaw cycles. Thermal polymerization was then conducted under vacuum following the temperature program: 35 °C for 6 h, 60 °C for 4 h, 100 °C for 1 h, and 120 °C for 1 h. The composites were then washed briefly with $CHCl_3$ and EtOH and thoroughly dried at 90 °C for 24 h under air. The synthesis conditions for the PS–SBA-15 materials are the same but using the following reagent ratio: 229 mg Sty, 71 mg DVB, 16 mg AIBN, and 1.8 mL of CH_2Cl_2.

Solvent treatments

Exposure to organic solvents was performed using either chloroform (BDH, 99.8%) or toluene (Fisher, 99.5%). In a typical test, 100 mg of a given composite was heated at 60 °C in a round bottom flask equipped with a reflux condenser for 24 h in the presence of 40 mL of the organic solvent. The resulting materials where then recovered by filtration and thoroughly dried under air at 90 °C for 24 h. Composite materials treated with chloroform and toluene are denoted –C and –T, respectively.

Characterization

N_2 sorption isotherms were measured at −196 °C with a Quantachrome Autosorb 1-C instrument. The composite materials were outgassed at 80 °C for 6 h prior to analysis. Specific surface area, S_{BET}, has been determined using the BET equation in the range $0.05 \geq P/P_0 \geq 0.20$ and the total pore volume measured at $P/P_0 = 0.95$. Pore size distributions have been determined both using the classical BJH model based on macroscopic thermodynamics and by using modern *non-local density functional theory* (NLDFT) approaches which consider interactions at the molecular level. In the latter case, both metastability (adsorption) and equilibrium models (desorption) that consider N_2 sorption at −196 °C in silica with cylindrical pore geometry are used for calculating pore size distributions and cumulative pore volumes [27, 28]. TG-DTA measurements were performed using a Netzsch STA 449C thermogravimetric analyzer, under air flow of 20 mL/min with a heating rate of 10 °C/min. FTIR-ATR spectra were recorded using a Nicolet Magna FTIR spectrometer with a narrow band MCT detector and a diamond ATR Golden-Gate accessory (Specac Ltd., London). The spectra were obtained from 128 scans with a resolution of 4 cm^{-1}. The deconvolutions of the carbonyl band were performed using the peak fitting tool in Grams/AI 8.0.

Results and discussion

Mesoporous PHEMA–silica composites

The N_2 sorption isotherms and the physicochemical characteristics of PHEMA–silica composites are presented in Fig. 1a and Table 1, respectively. The sorption and thermogravimetric data obtained for the PHEMA–SBA-15 material are consistent with previous reports [20, 25], indicative of uniform coating of PHEMA on the SBA-15 mesopore surface and high polymerization yields (>95%). Note that low angle powder X-ray diffraction (XRD) data obtained for the materials (not shown) are also consistent with previous data reported on similar materials [20, 25, 29]. This mesoporous PHEMA–SBA-15 composite material exhibits elevated specific surface area (387 m^2/g) and high pore volume (0.62 cc/g) despite the inclusion of 30 wt% of organic polymer. The pore size distributions (PSDs) were calculated either with the NLDFT model considering N_2 sorption at −196 °C in silica with cylindrical pores, or using the BJH algorithm (adsorption branch). The BJH model has also been selected to qualitatively illustrate pore size distributions in the 2–6 nm range. The pore size is estimated at 7.3 nm from both the NLDFT equilibrium model and the BJH method (adsorption branch). From the difference in pore size with the parent silica matrix (8.4 nm, from NLDFT equilibrium), the thickness of the coating is therefore estimated to be 0.55 nm. From the sorption isotherm, it can be seen that no dramatic changes in porosity occur upon solvent treatment, either using chloroform or toluene. The sharp H1 type hysteresis, characteristics of well-coated polymer–SBA-15 composites, is conserved indicating that the quality of the polymer coating is not altered and that the polymer component remains homogeneously distributed inside the pores of the SBA-15 host. However, slight variations can be found when comparing the data from Table 1. Specific surface area increases up to 480 and 462 m^2/g for materials treated in chloroform and toluene, respectively. Similarly, the total pore volume increases up to 0.75 and 0.78 cc/g for the materials treated in chloroform and toluene, respectively. These variations could apparently be due to the pore system of SBA-15 being less occupied by PHEMA, which in turn suggest that some of the polymer has been leached out during the treatment. However, no substantial variation in mass loss is observed by thermogravimetric analysis.

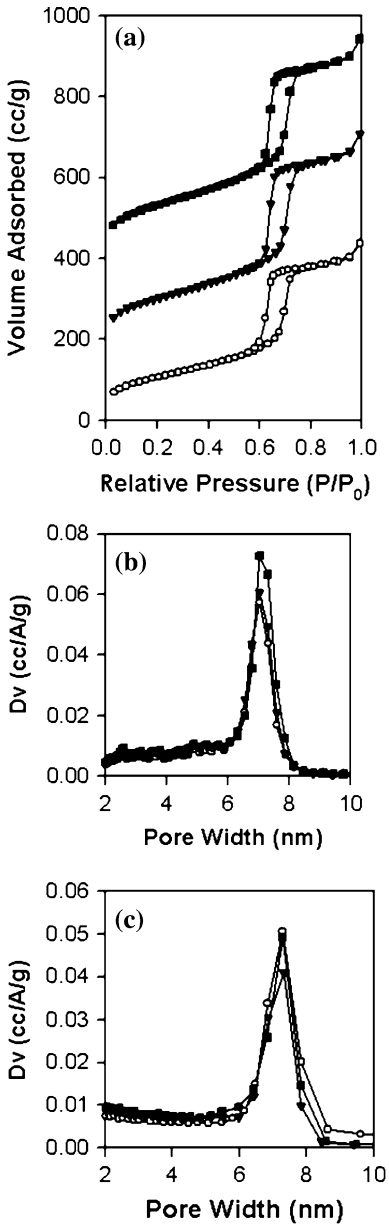

Fig. 1 **a** N_2 sorption isotherms at −196 °C of the different PHEMA–SBA-15 composites (20% cross-linking), **b** resulting NLDFT pore size distributions (metastability), and **c** resulting BJH pore size distributions [PHEMA (*circle*), PHEMA-T (*filled inverted triangle*), and PHEMA-C (*filled square*) composites]. The isotherms are offset by 175 and 400 cc/g, respectively

The porosity feature observed in the 2–6 nm regions is commonly associated with intrawall porosity and interconnections that are present in the pristine SBA-15 silica, originating from the interpenetration of ethylene oxide (EO) chains of the P123 block copolymer inside the silica matrix during synthesis [30]. This secondary porosity is of crucial importance for the synthesis of the polymer–mesoporous silica composites, since it is assumed to serve as the anchoring sites for the polymer moieties [20]. When taking a closer look at the PSDs, some differences seem to be visible in the 2–6 nm range (Fig. 1c). Compared to the untreated material, an increase in the volume derivative can be seen upon solvent treatment irrespective of the nature of the solvent used. This observation suggests that the polymer rearrange in some way upon solvent treatment to liberate a fraction of the intrawall porosity, which becomes

Table 1 Physicochemical characteristics of PHEMA- and PS-based composites (20% cross-linking) obtained from N_2 sorption, TG–DTA measurements and ATR-IR spectroscopy

Material	S_{BET} (m^2/g)	V_p[a] (cc/g)	w_a[b] (nm)	w_d[c] (nm)	w_b[d] (nm)	Mass loss[e] (%)	Bound carbonyls[f] (%)
PHEMA	387	0.62	7.0	7.3	7.3	24.5	56
PHEMA–C	480	0.75	7.0	7.3	7.3	24.0	58
PHEMA–T	462	0.78	7.0	7.3	7.3	23.4	58
PS	462	0.63	7.0	7.0	7.3	20.1	–
PS–C	547	0.78	7.0	7.0	7.3	19.2	–
PS–T	577	0.80	7.0	7.3	7.3	18.9	–

[a] Determined at $P/P_0 = 0.95$

[b] Obtained from the NLDFT metastability model (adsorption branch)

[c] Obtained from NLDFT equilibrium model (desorption branch)

[d] Obtained from the BJH algorithm (adsorption branch)

[e] Obtained from TG

[f] Obtained from ATR-IR deconvolutions

more important than for the untreated material. This intrawall pore volume remains, nevertheless, noticeably lower compared to the parent mesoporous silica host (not shown). This variation is coherent with the observed increase in specific surface area and pore volume (Table 1). For the PHEMA–SBA-15 composites, only materials prepared using BPO were considered in the present study since it had been established previously in the case of related PHEMA–inorganic systems that the use of AIBN instead of BPO led to no discernible differences [31].

TG–DTA measurements for the PHEMA composites are presented in Fig. 2. From these TG curves, almost no difference in mass loss is observed, indicating virtually no leaching of the polymer. However, the decomposition process is clearly delayed when the material is treated either with chloroform or toluene. A shift in the mass loss towards higher temperatures is observed and further evidenced when comparing the maxima in DTA (Table 2), which rise from 342 to 360 °C and 372 °C for toluene and chloroform, respectively. This higher thermal stability could be associated to enhanced polymer–silica interactions, which will be substantiated later below by ATR-IR. Based on our results, the following hypothesis may be formulated: PHEMA having high surface area could swell moderately in the presence of the organic solvent, despite being highly cross-linked, and then rearrange in such way that surface coverage is maximized. This rearrangement is thought then to enhance the interfacial polymer–silica interactions (van der Waals, hydrogen-bonding or confinement), resulting in enhanced stability of the PHEMA coating against thermal degradation.

A quite similar behavior is observed for the composites synthesized with a lower degree of polymer cross-linking (see Table 2, Fig. 2c). Note that the polymerization yields are slightly lower in the case of a reduced cross-linking degree (2%), as judged from the mass loss profiles

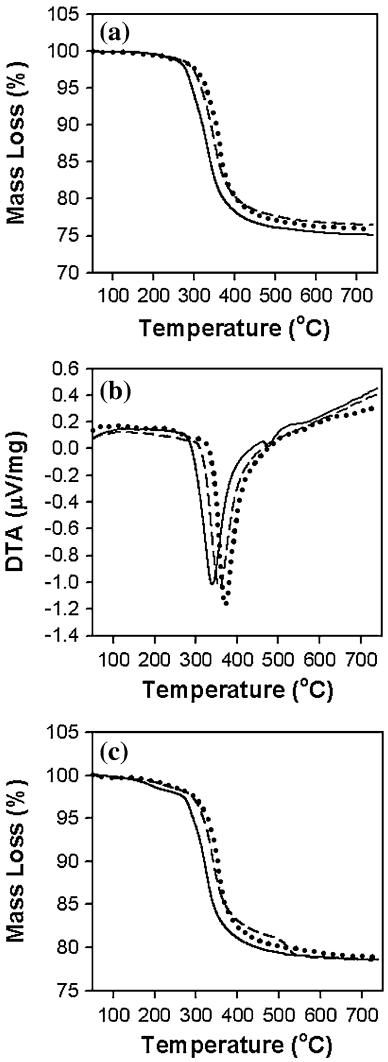

Fig. 2 **a** TG and **b** DTA curves of untreated (*solid*), chloroform-treated (*dotted*), and toluene-treated (*dashed*) PHEMA composites with 20% cross-linking; **c** TG curves of treated and untreated PHEMA composites with 2% cross-linking

Table 2 DTA results (peak maxima in °C) obtained from measurements for the PHEMA and PS (lower peak) composites upon solvent treatment

Material	Cross-linking degree (%)		
	20	5	2
PHEMA	342	330	325
PHEMA–C	360	359	338
PHEMA–T	370	348	336
PS	350	322	328
PS–C	350	328	341
PS–T	338	331	383

indicating lower organic content. The composites with low cross-linking generally show slightly lower degradation temperatures (i.e., lower thermal stability), being 330 and 325 °C for 5 and 2% materials, respectively. However, our data provide evidence that the polymer coating is sufficiently stable in organic solvent also at lower cross-linking degrees. From these sets of data, it is obvious that the maximum in DTA is also shifted to higher temperatures when the materials are treated with $CHCl_3$ or toluene. However, the observed effect of an improved thermal stability upon solvent treatment is slightly less pronounced than in the case of high cross-linking (20%) (Table 2). Interestingly, an additional process is visible between 400 and 500 °C for the 2% cross-linked PHEMA composite treated with toluene, which may be attributed to some solvent entrapment. Further investigations are under way to substantiate this effect.

Rearrangement upon solvent treatment is further evidenced by ATR-IR (Fig. 3A). The ATR-IR method can provide very reproducible measurement conditions for solid samples combined with high resolution [32]. This method is also particularly suitable for the characterization of functionalized mesoporous powders. The carbonyl band of PHEMA composites centered at 1,725 cm^{-1} is believed to arise from the contribution of carbonyls with different environments: free carbonyls (1,735 cm^{-1}) and carbonyls H-bonded (1,715 cm^{-1}) to surface silanols of the silica host [33]. Deconvolution of this carbonyl band allows us to determine the relative ratio of the two types of environments present in PHEMA–SBA-15 composites, as presented in Table 1. One can see that the bound to unbound carbonyls ratio slightly, but reproducibly, increase from 56 to 58% upon solvent treatment. This evolution further supports the hypothesis that rearrangement could be induced by solvent treatment, leading to greater PHEMA–silica interaction, and thus an increase in thermal stability.

Mesoporous PS–silica composites

The N_2 sorption isotherms and the physicochemical characteristics of PS–silica composites are presented in Fig. 4 and Table 1, respectively. The sorption and thermogravimetric data obtained for the PS–SBA-15 material are also consistent with data described in previous reports [20, 25], indicative of uniform coating of PS on the SBA-15 mesopore surface and high polymerization yields (>90%). Powder XRD data (not shown) are consistent as well with previous data reported on similar materials [20, 25]. The mesoporous PS–SBA-15 composite material exhibits high specific surface area (429 m^2/g) and high pore volume (0.79 cc/g) despite the inclusion of 30 wt% of organic polymer. The pore size is estimated at 7.0 nm using the NLDFT equilibrium model (7.3 nm from BJH using the adsorption branch). From the difference in pore size with the parent silica matrix (8.4 nm, from NLDFT equilibrium), the thickness of the coating is therefore estimated to be 0.7 nm, being apparently larger than the PHEMA coating. Solvent effects are expected to be quite different with the PS composites from those observed with PHEMA,

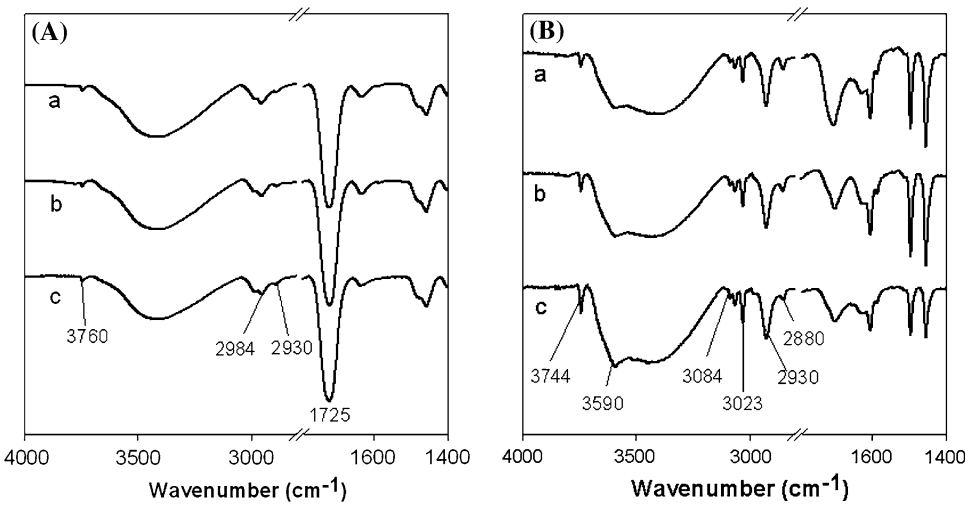

Fig. 3 ATR-IR spectra of **A** PHEMA–SBA-15 and **B** PS–SBA-15 composites (a) $CHCl_3$-treated; (b) toluene-treated; and (c) untreated

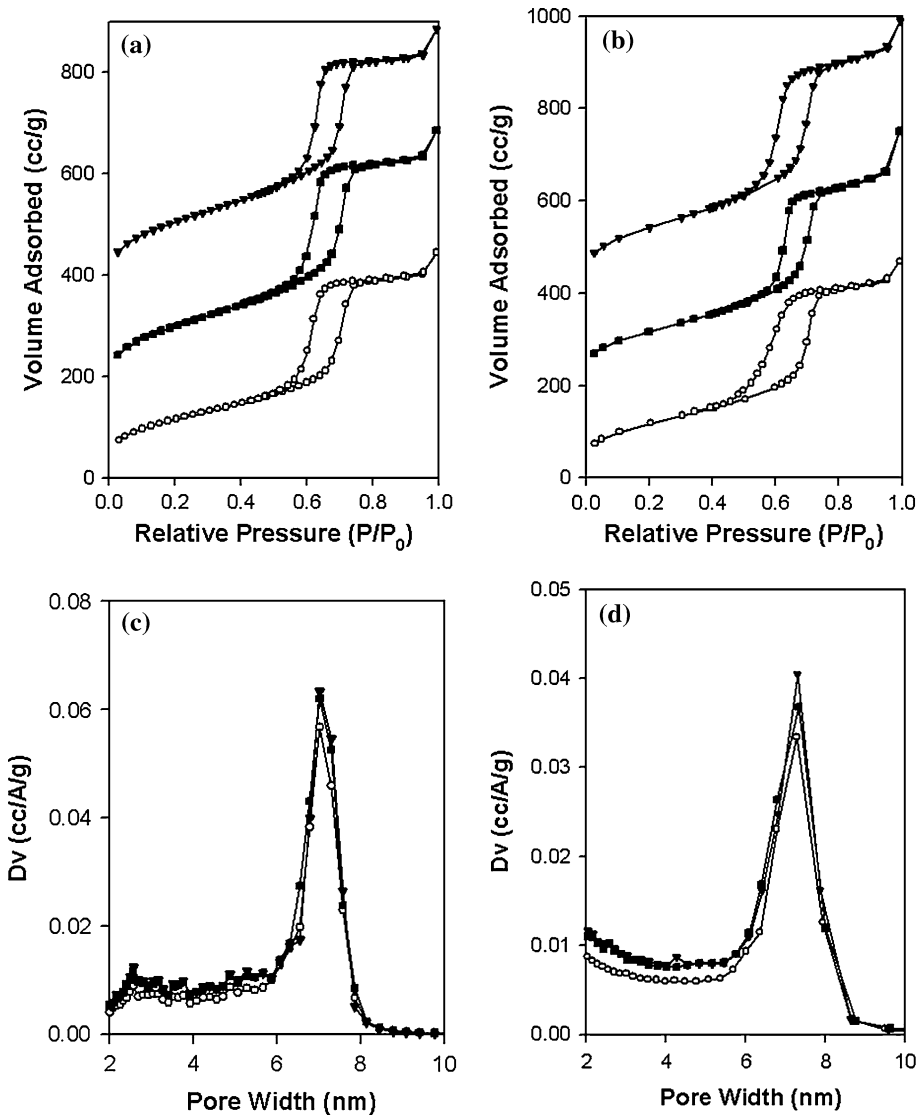

Fig. 4 **a** N_2 sorption isotherms at −196 °C of PS (AIBN)–SBA-15 composites (20% cross-linking); **b** N_2 sorption isotherms at −196 °C of PS (BPO)–SBA-15 composites; **c** resulting NLDFT (metastability) pore size distributions (PS-AIBN); and **d** BJH pore size distributions of PS (AIBN)–SBA-15 composites [PS (*circle*), PS–T (*filled square*), and PS–C (*filled inverted triangle*) composites). The isotherms are offset by 250 and 500 cc/g, respectively

first because the silica–PS interactions through hydrogen-bonding between silanols and aromatics [34] are expected to be weaker than the carbonyl–silanols interactions present in the PHEMA–silica composites, and second, because the intra-macromolecular interactions in PS are also considered weaker compared to carbonyl–hydroxyl hydrogen-bonding within PHEMA. One could thus expect the polymer to have an increased mobility and flexibility, which might eventually account for enhanced solvent effects. Such an effect is clearly seen for PS composites synthesized using BPO as a radical initiator: the N_2 sorption isotherms shown in Fig. 4b reveal that the solvent treatment induces distinct changes in the hysteresis loop, which becomes narrower. These observations suggest that treatment with either toluene or chloroform could be a suitable way to improve the homogeneity, and therefore the quality of the PS coating in SBA-15-type silicas when BPO is used as the radical initiator. Differently, little difference on the hysteresis is observed for PS-(AIBN)–SBA-15 composites (Fig. 4a). It can be seen from Table 1 that variations in surface area and pore volume occur as well upon treatment of PS-(AIBN)–SBA-15 composites with organic solvents, and these variations are quite similar to those observed for PHEMA. Specific surface area increases up to 547 and 577 m^2/g for chloroform and toluene, respectively, while the total pore volume increases slightly up to 0.78 cc/g for the PS–C sample and 0.80 cc/g for the PS–T material. A slight increase in pore size from 7.0 to 7.3 nm (from the PSD calculated using the NLDFT equilibrium model, Table 1) is observed for PS–T, which may be attributed to a more uniform PS surface coating along the mesopores obtained after organic solvent treatment. The PSD obtained from BJH are presented in Fig. 4d. As described previously for the PHEMA composites, an increase in volume derivative is similarly observed for the treated composites. Here again, swelling of the polymer, despite high cross-linking,

followed by reorganization of the polymer–silica interfaces may be the cause for the observed differences in intrawall porosity and the modulation in mesopore uniformity.

The thermal stability of treated and untreated PS composites has also been investigated by TG–DTA and the results are presented in Fig. 5. In contrast to the PHEMA composites, the decomposition of PS composites involves two processes, i.e., the formation of primary char (with DTA maximum around 350 °C), then its degradation at higher temperature [35, 36]. From the TG curves of the materials with 20% cross-linking, one can observe no important decrease in mass loss, which implies that almost no polymer leaching would take place. In contrast to PHEMA, no shift in the maximum of the DTA curves is observed upon treatment with both solvents. Although

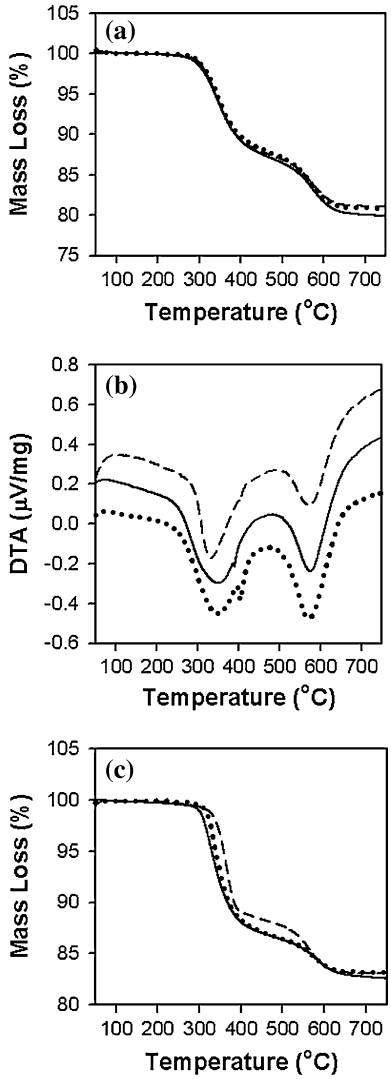

Fig. 5 **a** TG and **b** DTA curves of untreated (*solid*), chloroform-treated (*dotted*), and toluene-treated (*dashed*) PS composites with 20% cross-linking; **c** TG curves of 2% cross-linked treated and untreated PS (AIBN) composites

exposure to organic solvent helps to increase the surface area and the pore volume of the composite, it does not modify thermal stability. Similarly, no significant change is observed in the ATR-IR spectra (Fig. 3B). In particular, the peak at 3,590 cm^{-1}, which is attributable to silanols interacting with PS aromatic rings [34], is not varying in intensity relative to the peaks originating from the C–H vibrations of aromatics (3,084 and 3,023 cm^{-1}), suggesting that the silica–PS interactions are not altered upon solvent treatment.

In general, reducing cross-linking of polystyrene from 20 to 5 and 2% in the material leads to a lower thermal stability of the PS–SBA-15 composites. One can see from Table 2 that the DTA maximum shifts from 350 to 322 and 328 °C for 5 and 2% of cross-linking, respectively. The solvent treatments affect strongly the decomposition temperature of the composites prepared with the lower cross-linking degree. In particular, the TG curves of materials with 2% clearly shifts to higher temperatures, reflected by a higher DTA maximum of 341 °C for $CHCl_3$ and 383 °C for toluene, being more than 50 °C higher in the latter case. This might be attributable to a higher swelling of the lower cross-linked polymer, which might cause a more favorable rearrangement. Again, differences in the TG profile of PS–T in the 400–550 °C temperature range seem to suggest possible polymer modification and/or solvent entrapment.

Conclusion

Exposure to organic solvents for mesoporous PHEMA–SBA-15 and PS–SBA-15 materials appears as a possible method to improve some of the properties of these composites. Clearly, different effects are observed depending on the nature of the polymer introduced in SBA-15 silica. In the case of PHEMA, treatment with chloroform or toluene resulted in an increased thermal stability of the materials, which may be due to enhanced silica–PHEMA interactions. We may attribute this behavior to sufficient swelling of the polymer, irrespective of the nature of the solvent, allowing for polymer rearrangement on the mesopores surface and in the walls. The size and shape of the main mesopores does not seem to be affected by the treatment, the pore condensation behavior being similar before and after treatment. On the other hand, the treatment of the PS–SBA-15 composite with either chloroform or toluene resulted in a small variation of the mean pore size, probably also caused by reorganization of the polymer–silica interface, which here improved the uniformity of the polymer coating. When BPO is used as radical initiator, the resulting materials exhibit modified pore size and shape, as evidenced by slightly different pore condensation behavior. However, no improvement of the thermal stability could be

observed for PS–SBA-15. Lowering the cross-linking degree for both polymers resulted generally in a slight decrease in thermal stability of the composites, which remain sufficiently high even with only 2% cross-linking. Although confirmation of the observed sorption behaviors and intrawall porosity variations is still needed with argon sorption measurements at 87 K [28], we may conclude now that the treatment of polymer–mesoporous silica composites with organic solvent seems to provide an simple method for improving the homogeneity of the polymer coating, and thus quality of the materials. In addition, a detailed structural characterization of the mesoporous composites using high-resolution powder X-ray diffraction (XRD) and transmission electron microscopy (TEM) is currently ongoing and will be reported shortly in a separate study.

Acknowledgements Financial support from the Natural Sciences and Engineering Research Council of Canada (NSERC) and le Fonds Québécois de la Recherche sur la Nature et les Technologies (FQRNT) are gratefully acknowledged. The authors wish to thank Prof. Michel Pézolet and Jean-François Rioux for the access to ATR-IR measurements (Chemistry Department, Laval University).

References

1. Beck JS, Vartuli JC, Roth WJ, Leonowicz ME, Kresge CT, Schmitt KD, Chu CTW, Olson DH, Sheppard EW, McCullen SB, Higgins JB, Schlenker JL (1992) J Am Chem Soc 114:10834
2. Zhao D, Huo Q, Feng J, Chmelka BF, Stucky GD (1998) J Am Chem Soc 120:6024
3. Ying JY, Mehnert CP, Wong MS (1999) Angew Chem Int Ed 38:56
4. Thomas JM (1999) Angew Chem Int Ed 38:3589
5. Taguchi A, Schuth F (2005) Microporous Mesoporous Mater 77:1
6. Tiemann M (2007) Chem Eur J 13:8376
7. Hartmann M (2005) Chem Mater 17:4577
8. Vallet-Regi M, Balas F, Arcos D (2007) Angew Chem Int Ed 46:7548
9. Wight AP, Davis ME (2002) Chem Rev 102:3589
10. Kickelbick G (2004) Angew Chem Int Ed 43:3102
11. Yoshitake H (2005) New J Chem 29:1107
12. Hoffmann F, Cornelius M, Morell J, Fröba M (2006) Angew Chem Int Ed 45:3216
13. Stein A (2003) Adv Mater 15:763
14. Wu CC, Bein T (1994) Science 264:1757
15. Moller K, Bein T, Fischer RX (1998) Chem Mater 10:1841
16. Cho MS, Choi HJ, Kim KY, Ahn WS (2002) Macromol Rapid Commun 123:713
17. Acosta EJ, Carr CS, Simanek EE, Shantz DF (2004) Adv Mater 16:985
18. Molenkamp WC, Watanabe M, Miyata H, Tolbert SH (2004) J Am Chem Soc 126:4476
19. Rosenholm JM, Penninkangas A, Linden M (2006) Chem Commun 3909
20. Choi M, Kleitz F, Liu D, Lee HY, Ahn WS, Ryoo R (2005) J Am Chem Soc 127:1924
21. Zhang Y, Zhao L, Lee SS, Ying JY (2006) Adv Synth Catal 348:2027
22. Zhang L, Abbenhuis HCL, Gerritsen G, Bhriain NN, Magusin PCMM, Mezari B, Han W, van Santen RA, Yang Q, Li C (2007) Chem Eur J 13:1210
23. Fuertes AB, Tartaj P (2007) Small 3:275
24. Tian BS, Yang C (2009) J Phys Chem C 113:4357
25. Marcoux L, Kim TW, Bilodeau S, Kleitz F (2007) Stud Surf Sci Catal 170:1836
26. Choi M, Heo W, Kleitz F, Ryoo R (2003) Chem Commun 1340
27. Ravikovitch PI, Neimark AV (2001) J Phys Chem B 105:6817
28. Thommes M (2004) Nanoporous materials; science and engineering. ICP, London, UK
29. Rosenholm JM, Czuryszkiewicz T, Kleitz F, Rosenholm JB, Lindén M (2007) Langmuir 23:4315
30. Galarneau A, Cambon H, Di Renzo F, Ryoo R, Choi M, Fajula F (2003) New J Chem 27:73
31. Aydin B, Bilodeau S, Hamidipour M, Larachi F, Kleitz F (2008) Ind Eng Chem Res 47:2569
32. Boulet-Audet M, Lefevre T, Buffeteau T, Pezolet M (2008) Appl Spec 62:956
33. Landry CT, Coltrain BK, Wesson JA, Zumbulyadis N, Lippert JL (1992) Polymer 33:1496
34. Onida B, Allian M, Borello E, Ugliengo P, Garrone E (1997) Langmuir 13:5107
35. Levchik GF, Si K, Levchik SV, Camino G, Wilkie CA (1999) Polym Degrad Stab 65:395
36. Van Krevelen DW (1975) Polymer 16:615